**IRAQI BULLETIN OF GEOLOGY AND MINING (IBGM)\
IRAQ GEOLOGICAL SURVEY (GEOSURV-IRAQ)**

Vol.18, No.2, 2022 ***p 1 – 24***

THE MID – MIOCENE CLIMATIC OPTIMUM (MMCO) MANIFESTATION IN IRAQ: CARBON AND OXYGEN ISOTOPES PROXIES

Mustafa A. Ali[1]*, Sa'ad Z. Al-Mashaikie[2] and Arsalan A. Othman[3]

Received: 03/ 08/ 2022, Accepted: 16/ 11/ 2022
Keywords: Stable isotope; Jeribe Formation; Monterey excursion; Miocene; Palaeoceanography

ABSTRACT

The present paper deals with the variability of the primary isotopic composition of seawater in the shallow water zone. Sedimentary successions of middle Miocene outcropping in the eastern part of Iraq provide an excellent archive of the oxygen and carbon isotopes. We analyzed the $\delta^{13}C$ and $\delta^{18}O$ to investigate the relationship between the lithostratigraphic units and the deviation of the stable isotopes. The results show a significant relationship between the depositional energy changes and both $\delta^{13}C$ and $\delta^{18}O$ composition. That displays the details of oxygen isotope events (Mi-events) and additional information about Mi2 and 3 zones, reflecting significant changes in the glaciation period, which have minor steps (interglacial period). At the same time, carbon isotope maxima (CM-events) reflect changes in organic carbon burial and refine the Monterey Excursion. Facies analysis revealed several microfacies could be distinguished, reflecting depositional environments including; supratidal and intertidal, lagoon, patch-reef, and open marine environments, matching with their isotopes storage differential, enhancing ^{13}C and high rates of sedimentation in deeper facies. The stable isotopes ($^{18}O/^{16}O$ and $^{13}C/^{12}C$) provide an excellent archive of the Neogene (middle Miocene Transgression) 's paleoceanography for the Neo-Tethys. Oxygen and carbon isotopic stratigraphy for bulk rock were analyzed to distinguish Monterey Event and climate optima.

INTRODUCTION

Previous works have been surveyed, including petrographic studies of the Jeribe Formation. However, only two old studies utilize the traditional geochemical parameters of the formation in Mosul and western desert regions to understand and interpret the depositional environment. On the other hand, there are no more studies of the Jeribe Formation from the point of stable isotopes view of C and O to define the global Monterey excursions events. Therefore, it is worth mentioning that the present paper relies on all detailed geological mapping data for an area, from GEOSURV, the definition of the exposed formations and their extensions.

[1] Department of Geology, Al-Andalus Square, Baghdad 10068, Iraq,
e-mail: mustafaasaad82@gmail.com
[2] Department of Geology, College of Science, University of Baghdad, Baghdad, Iraq
[3] Iraq Geological Survey, Al-Andalus Square, Baghdad 10068, Iraq;
ORCID iD: 0000-0002-4212-228X; e-mail: arsalan.aljaf@gmail.com

One of climate history events' most common global features is the long-lasting positive carbon-isotope excursion or "Monterey Excursion". The global Monterey excursions are recognized in many deep-sea and, recently, in shallow-water depth records during the Miocene epoch. However, despite their importance to global climate evolution, they have never been recorded in shallow marine carbonate successions in Iraq. The Monterey excursions have a significant disturbance with a $\delta^{13}C$ shift toward heavier values. Woodruff and Savin (1991) were the first researchers to record the events of Monterey excursions and recognize the internal periodic variation in the $\delta^{13}C$. They defined six so-called carbon isotope maxima (CM-events). The Shift of $\delta^{13}C$ to heavier values is recognized in many deep-sea locations. Recently, it has been recorded during Miocene at ~17.5 Ma, terminating at ~13.5 Ma in shallow water depth (Auer *et al*., 2015; Corfield and Cartlidge, 1993; Flower and Kennett 1993, 1994, 1995; Mourik *et al*., 2010; Rea, Snoeckx, and Joseph, 1998; Smart and Murray, 1994; Vincent and Berger, 1985). Isotopic studies on the shallow marine carbonates of the Miocene have revealed evidence for paleo-tectonic (Armstrong-Altrin *et al*., 2009; Kumar *et al*., 2002; Madhavaraju *et al*., 2004; Maheshwari *et al*., 2005; Marquillas *et al*., 2007; Nagarajan *et al*., 2008) and global scale tectonic events (Amodio *et al*., 2008; Gröcke *et al*., 2005; Maheshwari *et al*., 2005).

The Monterey Formation in California shows dramatic increases in organic carbon accumulation in Pacific Rim sediments linked to invigorated coastal and equatorial upwelling of high carbon and oxygen content (Vincent and Berger, 1985; Woodruff and Savin, 1991). The significant positive carbon isotope shift is generally used to establish the global organic carbon budget during oceanic anoxic events. For example, Scholle and Arthur (1980) suggested that the volume of organic carbon (C_{org}) buried was a sizable part of the global carbon budget.

Miller and Katz (1987); Flower and Kennett (1994); Zachos *et al.* (2001); Billups and Schrag (2003); Holbourn *et al.* (2007); and Diester-Haass *et al.* (2013) considered the major climatic shift during the Neogene is marking for the beginning of the gradual transition from the middle Miocene into the icehouse climate of the Pleistocene. Miller and Katz (1987); Diester-Haass *et al.* (2013), and Billups and Schrag (2003) used the benthic foraminiferal accumulation from Deep Sea Drilling Project in different sites, Hole 588 in the Pacific and Southern Oceans, Sites 558 and 563 in North Atlantic, and 757 and 689 from the subtropical Indian Ocean and the Weddell Sea, respectively, showed a distinct productivity maximum during CMs and linked their occurrences to the time of major expansion of ice on Antarctica. Woodruff and Savin (1991) stated a similar conclusion about the carbon isotope maxima recorded in Ocean Drilling Program Site 747. Similar events were recorded for oxygen isotope data during the Miocene (Auer *et al*., 2015; Chaproniere 1981; Cooke *et al*., 2008; Diester-Haass *et al*., 2013).

The Miocene oxygen isotope events (Mi-1–Mi-7) were globally concurrent and are related to the change in paleo-climate. These events were named by Scott *et al*. (1995) as glacial zones indicating global cooling. Miller *et al.* (1991), Miller *et al.* (1991); Wright *et al.* (1992), Westerhold *et al.* (2005), and Chakrabarti *et al.* (2011) described several extreme glacial events from $\delta^{18}O$ records, called Mi zones and linked Mi1to Mi4 zones to the East Antarctic ice sheet expansion, while Mi5, Mi6, and Mi7 zones were associated with the ice volume accumulation on the western part of Antarctica through the middle-late Miocene. Cooling or glacial prominent period occurs synchronously with CM events (Sosdian *et al*., 2020 and refernce in there).

Numerous published studies stated that the positive relation indicates a global $\delta^{13}C$ excursion coincides with $\delta^{18}O$ increased value, which is more significant in cool deep water. Sosdian *et al.* (2020) proposed that these events are associated with elevated oceanic dissolved inorganic carbon caused by volcanic degassing and organic carbon burial caused by sea-level rise on drowned continental shelves. He has documented a positive carbon isotope excursion ($\delta^{13}C$) of the global ocean's records in planktonic and benthic foraminifera. Moreover, these events have been reported in carbonates by Auer *et al.* (2015) as evidenced by plankton-rich in Mi3a and Mi3b reflecting increases of upwelling-induced nutrient availability, Mi2a is dominant in siliceous plankton and sponges records, while Mi2b coincides with phosphate hardground records.

Edgar *et al*. (2015) linked the enrichment of heavy carbon in the surface waters to the high productivity of the photic zone would preferentially remove ^{12}C by photo symbionts and phytoplankton, leaving the ambient seawater enriched at ^{13}C. While below the photic zone, values of the ^{12}C are increased relative to surface waters as a function of reducing photosynthetic activity and re-mineralizing ^{12}C. Raymo *et al*. (1988) and Ruddiman *et al*. (1997) linked the enrichment of heavy carbon to chemical weathering from continental arc. These events are virtually unrecognized in shallow marine carbonates. Overall, these documents are derived primarily from cooling, exist in open marine and shelf settings, reflect slope settings and recorded higher $\delta\ ^{18}O$ values due to more great basinal water masses (Miller *et al*., 1991; Woodruff and Savin 1989) and for open ocean shallow-dwelling planktonic species, which is enrichment in ^{13}C by up to 4‰ compared to other settings. According to Immenhauser *et al.* (2002), water masses down to about 150 m depth documented isotopically light meteoric water ^{18}O in the modern surface sediments of Great Bahama Bank. Swart and Eberli (2005) mentioned the absence of variations in $\delta^{13}C$ irrespective of change of facies type.

In the current study, we show values variability composition of ^{13}C and ^{18}O concerning their differences over facies change. Due to the severely limited interpretation of the stable-isotope record of shallow water carbonates, the main objective of this study was to examine the variability of the primary isotopic composition of seawater in this setting and detailed interpretation of the Miocene isotope events and to link their occurrences to lithological record.

REVIEW OF GEOLOGY AND STRATIGRAPHY

Bellen *et al*. (1959) described the Jeribe Formation (Middle Miocene) for the first time from the type locality that comprised a 173 m thick rock sequence in the Sinjar anticline. The Middle Miocene Jeribe Formation belongs to tectonostratigraphy Megasequence A11, which involves several formations (Figure 1). It considers a new transgressive stage in the foredeep shelf margin (Jassim and Goff, 2006). The formation was controlled by the "Savian" continental collision movement between Arabian and Eurasian plates affecting the foreland basin (Jassim and Goff 2006; Numan 1997). Jeribe Formation was deposited in two main basins, i.e., Mosul and Kirkuk blocks (Jassim and Goff, 2006). Aqrawi *et al*. (2010) described the Miocene sequence, microfacies, and depositional environment of the Jeribe Formation. Fouad (2012) stated that the Jeribe Formation was deposited in the outer platform margin.

Stable isotopes of $\delta^{13}C$ and $\delta^{18}O$ of the Jeribe carbonates were recorded for the first time by Ali and Sa'ad (2018). They concluded variation composition on both $\delta^{13}C$ and $\delta^{18}O$ was controlled by sea-level oscillation. Depletion of $\delta\ ^{13}C$ and $\delta\ ^{18}O$ isotopes is controlled by lowering the sea level, which is restricted to shallow marine facies, while the enrichment of

$\delta\ ^{13}C$ and $\delta\ ^{18}O$ isotopes is controlled by sea-level rise. Furthermore, they identified that paleo-depth involves mixed layer and thermocline layer inference by enrichment and depletion of the stable isotopes. Jeribe Formation represents the last deposited marine sediments before the final closure of the southern New-Tethys Sea. In the study area, the formation is exposed as relics along the thrust fault and in the core of the Koolic anticline. It consists of thick dolomite beds. The upper and the lower contact is conformable with overlaid Fatha Formation and underlined Dihban Formation. The total thickness of the formation is 70 m.

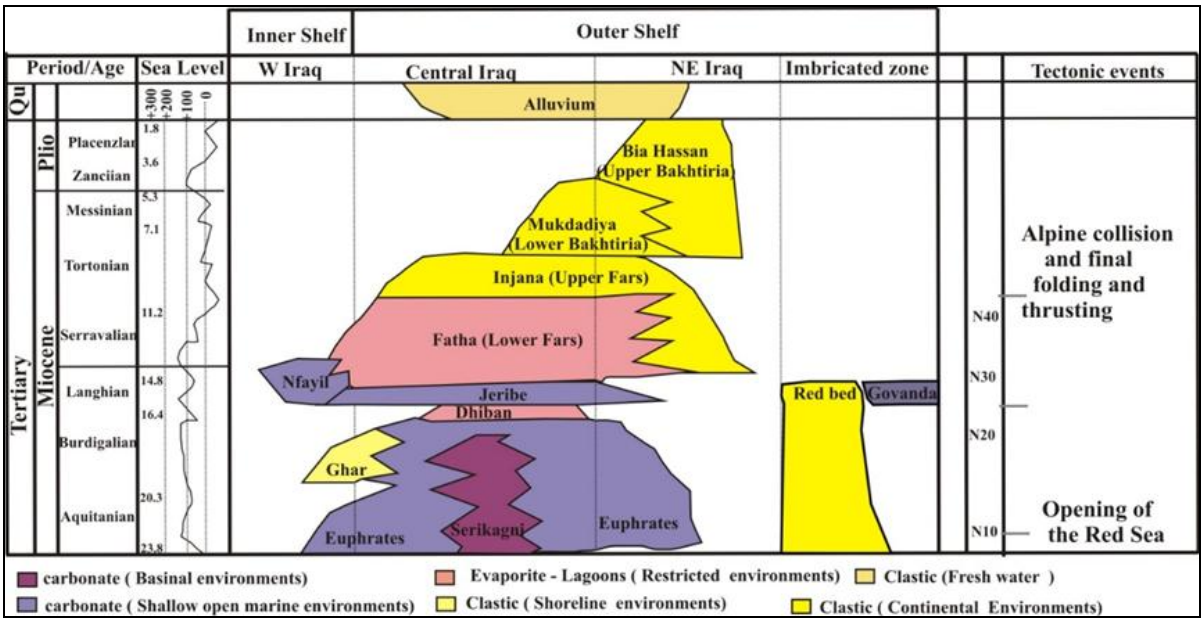

Fig.1: Chronostratigraphy of Miocene formations in Iraq
(modified after Jassim and Goff, 2006)

METHODS AND MATERIALS

Detailed geological mapping of the study area was preceded by recovering two sections (Figures 2 and 3). For each section, field description was carried out, such as bed thickness, facies, sedimentary structures, and facies successions. Forty-two samples (at 2 – 3 m intervals) were collected from fresh surfaces of carbonate rocks, avoiding the late-diagenetic cracks, veins, weathered materials, and stylolites. Samples were cut perpendicular to the bedding plane to define the textures and mineralogical compositions and obtain the primary signature of isotopes based on the well-preserved texture. The first section (Ja) is located in the SW core flank of the Koolic-1 anticline, while the second section (Jb) is situated in the core of the Koolic-3 anticline in Showshareen valley. The selected sections represent an ideal column of the Kirkuk – Dezful Embayment (Figures 4, 5 and 6). Twenty samples were analyzed to determine the stable isotopes of C^{12-13} and O^{16-18} using acid conversion and IRMS. The instrument is a continuous Flow-Isotope Ratio Mass Spectrometry (CF-IRMS). Analyses were performed in the labs of Iso-Analytical Limited, United Kingdom. A modified version of Hudson's plots reproduced by Nelson and Smith (1996) has been used.

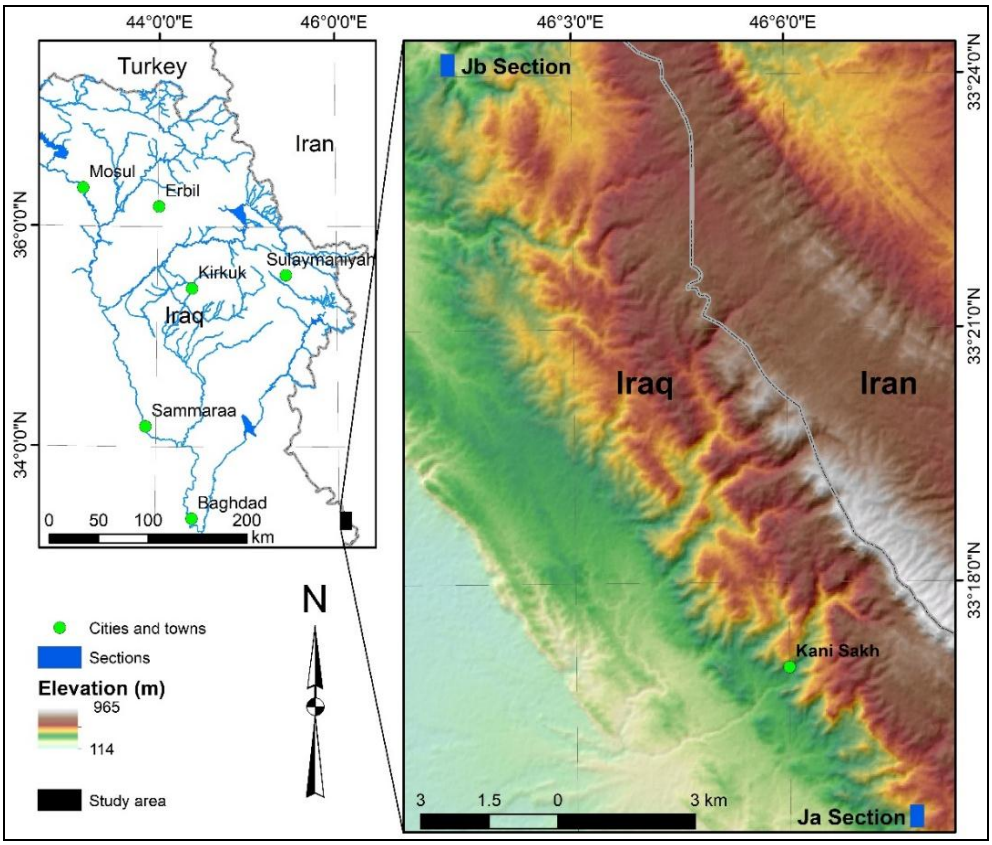

Fig.2: Map showing the location of the Ja and the Jb sections

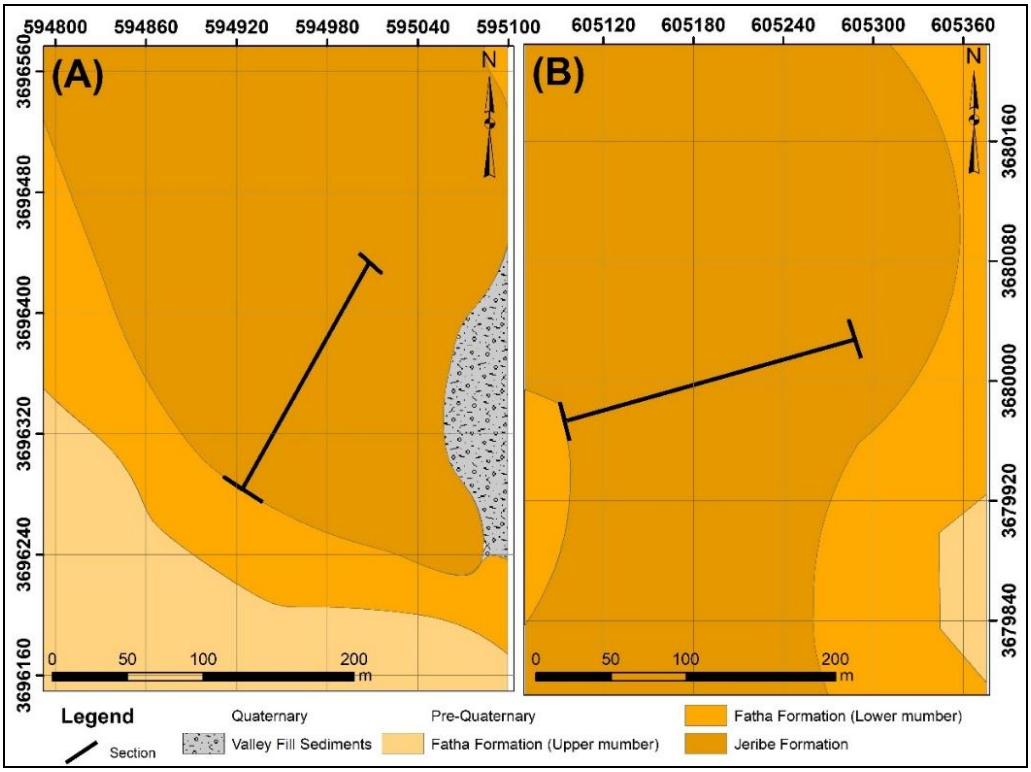

Fig.3: Geological maps of the study area showing the selected stratigraphic sections of (A) Jb and (B) Ja area

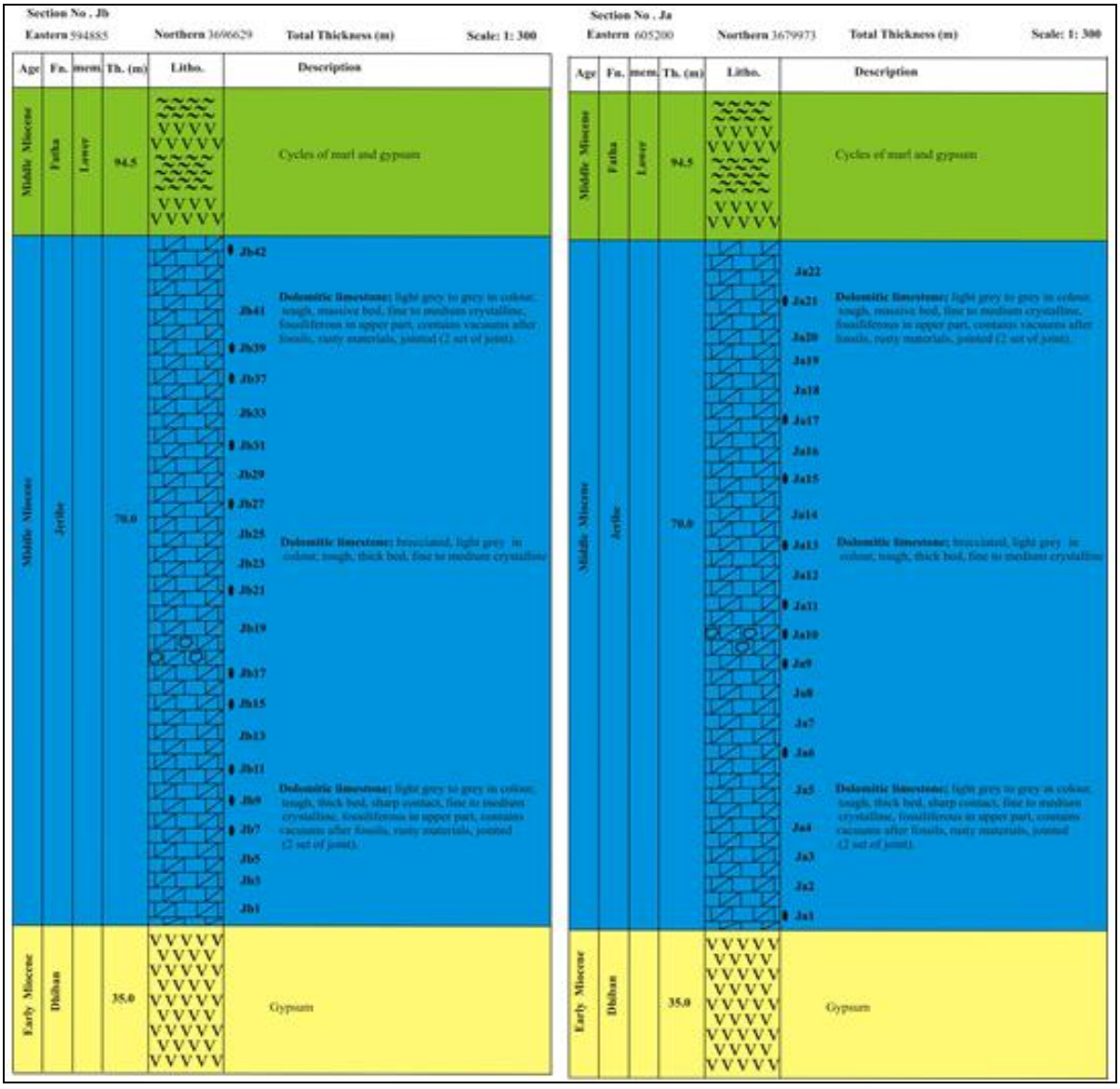

Fig.4: Stratigraphic logs with plots of sample locations
of the studied sections

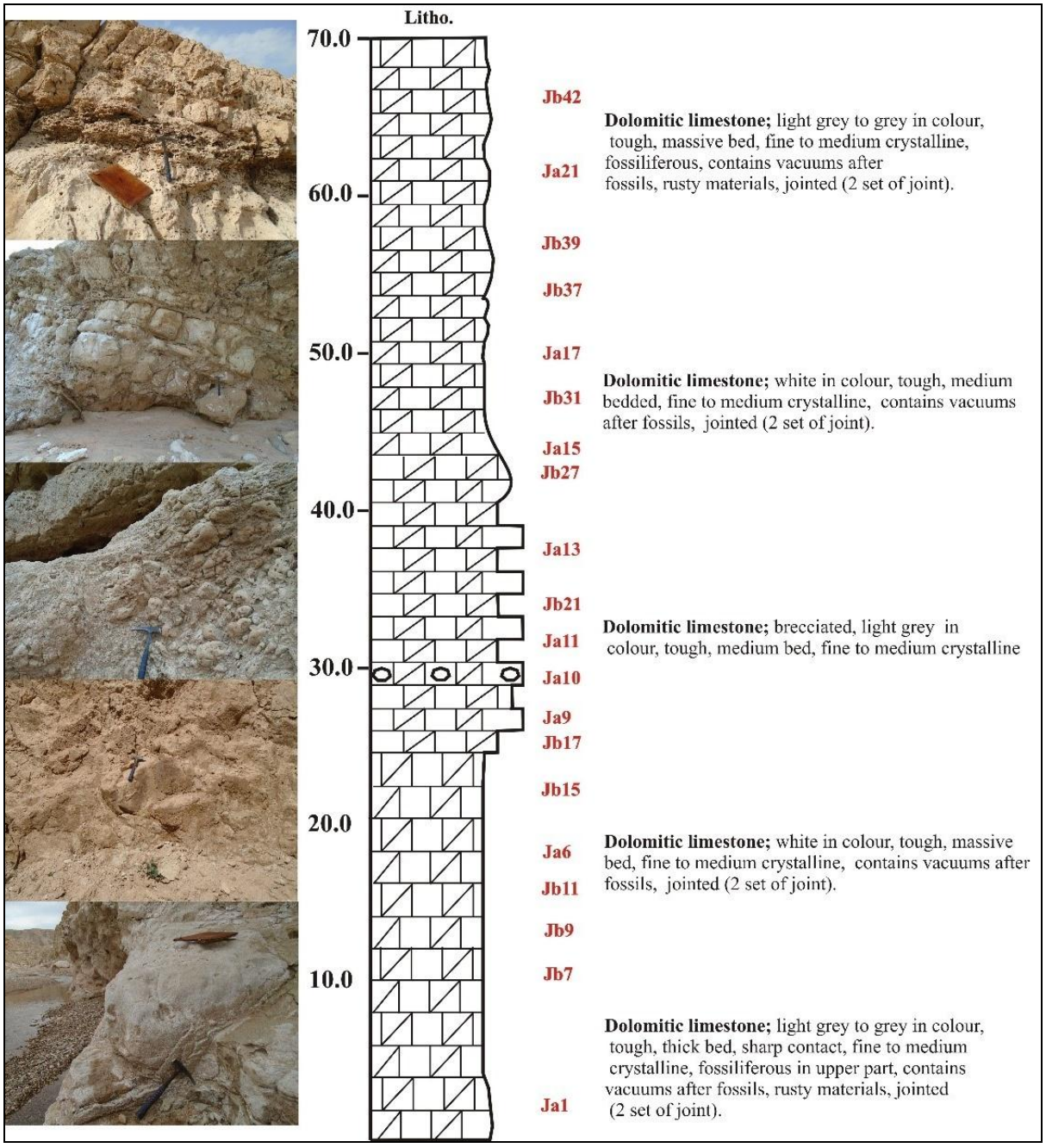

Fig.5: The ideal composite column from selected stratigraphic sections shows the vertical distribution of the selected samples based on the well-preserved texture

Fig.6: Field photographs of the Jeribe Formation in the studied localities
A and **B**: Sedimentary structure reflected Intretidal facies/ Fenestral porosity;
C: Sedimentary structure reflected Supratidal facies/ mudcrack;
D: brecciated bed occurred in the middle part of the formation.
E and **F**: Stromatolite

- **Carbon-13 and Oxygen-18 Isotopes Analysis**

Isotope analysis was carried out by first adding phosphoric acid to the samples in Clean Exetainer^{TM} tubes after flushing them with 99.9% helium for 3 hours at 90 °C and allowing them to settle overnight to complete the conversion of carbonate to CO_2. Reference and control materials were prepared in the same way. Next, the liberated CO_2 gas was analyzed by Continuous Flow-Isotope Ratio Mass Spectrometry (CF-IRMS). A double-holed needle collected carbon dioxide in ExetainerTM tubes into a continuously flowing stream. The CO_2 was resolved on a packed column gas chromatograph, which is carried forward into the ion source of a Europa Scientific 20 – 20 IRMS to ionize and accelerate. Gas isotopes of different

masses were separated in a magnetic field and simultaneously measured using a Faraday cup collector array to measure the isotopomers of CO_2 at m/z 44, 45, and 46. The phosphoric acid used for digestion had been prepared for isotopic analysis following Coplen *et al*. (1983).

- **Reference Standards and Quality Control**

The reference materials used for sample analyses were IA-R022 (Iso-Analytical working standard calcium carbonate, $\delta^{13}C_{V\text{-}PDB}$ = -28.63 ‰ and $\delta^{18}O_{V\text{-}PDB}$ = -22.69 ‰), NBS-18 (carbonatite, $\delta^{13}C_{V\text{-}PDB}$ = -5.01 ‰ and $\delta^{18}O_{V\text{-}PDB}$ = -23.20 ‰), IA-R066 (chalk, $\delta^{13}C_{V\text{-}PDB}$ = +2.33 ‰ and $\delta^{18}O_{V\text{-}PDB}$ = -1.52 ‰), and quality control. IA-R040 was used as an additional control. The dolomite powder has long-term mean scale corrected values for heavier (carbon 13 and oxygen 18) that have been documented over several years. The measured values for the check samples are provided in the results file. Acid preparations of samples and controls are measured directly against acid preparations of working calcium carbonate standard. This procedure eliminates separate corrections for temperature-dependent isotope fractionation. The results obtained for the NBS-18 and IA-R066 controls are used to check and correct data as required. IA-R022 has been calibrated against and is traceable to NBS-18 and NBS-19 (limestone, $\delta^{13}C_{V\text{-}PDB}$ = +1.95 ‰, and $\delta^{18}O_{V\text{-}PDB}$ = -2.2 ‰). IA-R066 has been calibrated against and is traceable to NBS-18 and IAEA-CO-1 (Carrara marble, $\delta^{13}C_{V\text{-}PDB}$ = +2.5 ‰ and $\delta^{18}O_{V\text{-}PDB}$ = -2.4 ‰). NBS-18, NBS-19, and IAEA-CO-1 are inter-laboratory comparison standard materials distributed by the International Atomic Energy Agency (IAEA).

RESULTS

Facies associations: The microfacies studied in forty-two thin-section. Based on textures and fossils assemblage of the carbonate rocks of Jeribe Formation reveals upward grading from the Intertidal (cf. laminated mudstone) to the semi-restricted lagoon, quiet environment (cf. bioclasts wackestone/ packstone), patch-inner ramp (cf. grainstone/ boundstone), supratidal/sabkha (cf. Domal Stromatolite) and open marine (cf. packstone), (Table 1). Carbonate grains are two main types, e.g., skeletal and non-skeletal grains. The skeletal grains have a biochemical origin and are formed as internal or external skeletal units of plants or animals.

Table 1: Main microfacies and depositional environments of Jeribe Formation

Facies Association	Microfacies type	Petrographic description	Th. (m)	Depositional environment
Lagoon	Bioclastic Peloid dolowackestone/ packstone & Algal dolowackstone	Red algae and benthic foraminifera (Milliods)	10	Moderate energy Semi-Restricted Lagoon
patch-reef	Coral Boundstone/ Grainstone	Coral with fewer algae and benthic foraminifera	6	Moderate energy Patch-reef
Sallow open marine	Foraminifer-bioclastic wackestone/ packstone & Bioclastic wackestone	Red algae and benthic foraminifera (Milliods, Soritidae, Alveolinidae species with Mollusc shells	35	Moderate to high energy Open shelf/ distal inner
Tidal Flat (Intertidal & Supratidal)	Unfossiliferous dolo Mudstone Algal dolowackstone Algal anhydritic dolo mudstone & Stromatolite Framestone	Laminated, red and green Algae & Domal Stromatolite, Densely laminated	15	Moderate energy Semi-Restricted/ Lagoon

The identified skeletal grains are represented by benthonic foraminifera, coral, red coralline algae, and calcareous algae: Dendritina sp. and Alveolinidae species, just Borelis melo sp, with shell fragments of Mollusca (gastropod).

Non-skeletal grains are formed by the diversity of physical and chemical processes; they are pellets, common grains in the shallow-marine tidal and subtidal shelf carbonates. Pellets are the main non-skeletal grains in packstone and less in the other depositional texture. Micrites of microcrystalline, neomorphosed to microspare, are the most common in the Jeribe Formation. Intraclasts are less common carbonate grains in the formation. Mainly based on Stratigraphic position (below and above formations) and assemblage fauna, the Jeribe Formation was attributed variously to the «Middle Miocene» (Figures 7, 8, 9, 10 and 11).

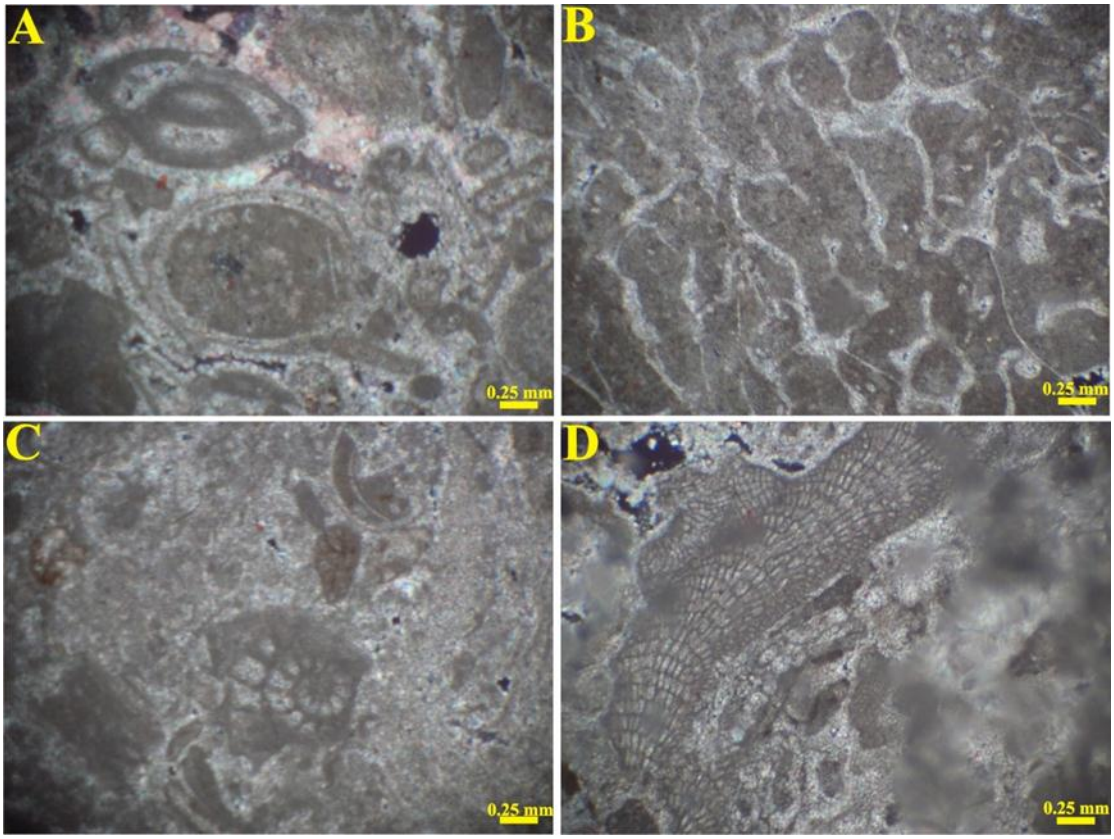

Fig.7: **A**: Benthic foraminifera/ Miliolids species/ Jb19, **B**: Binding of Coral/ Ja10, **C**: Benthic foraminifera/ Soritide species/ Jb25, and **D**: Coralline algae (red algae) Mesophyllum sp./ Ja9

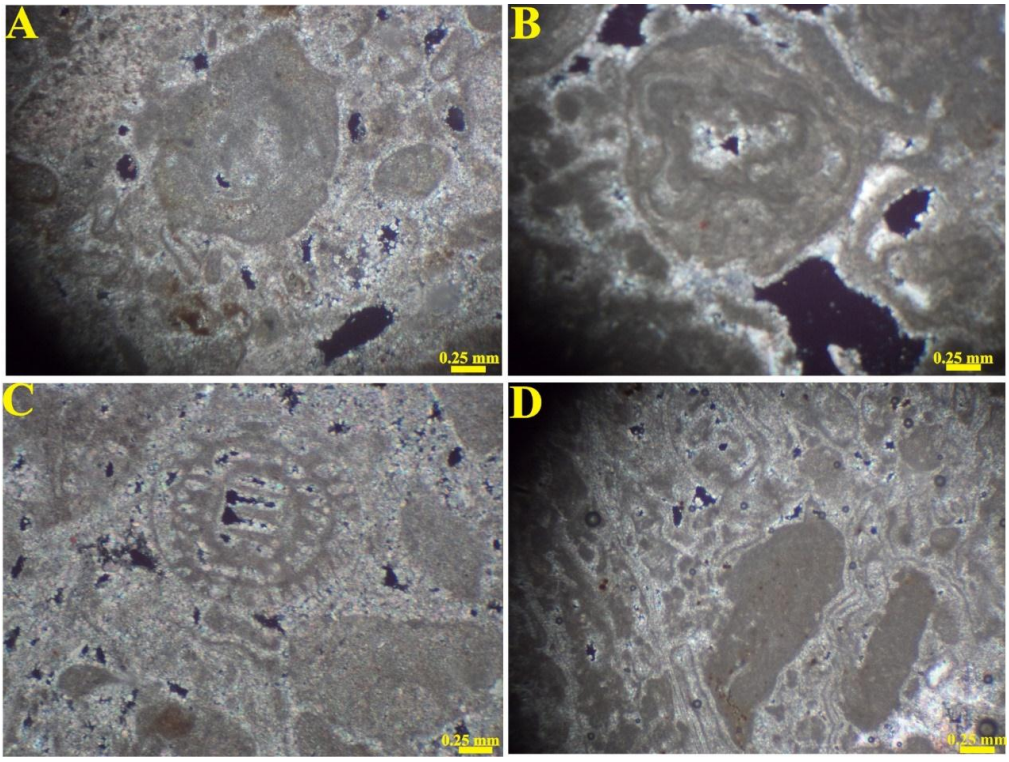

Fig.8: **A**: Binding of Coralline algae/ Jb31, **B**: Domal stromatolites/ Ja20, **C**: Dasycladaceae green algae/ Jb3, and **D**: Binding of Coralline/ Jb19 algae

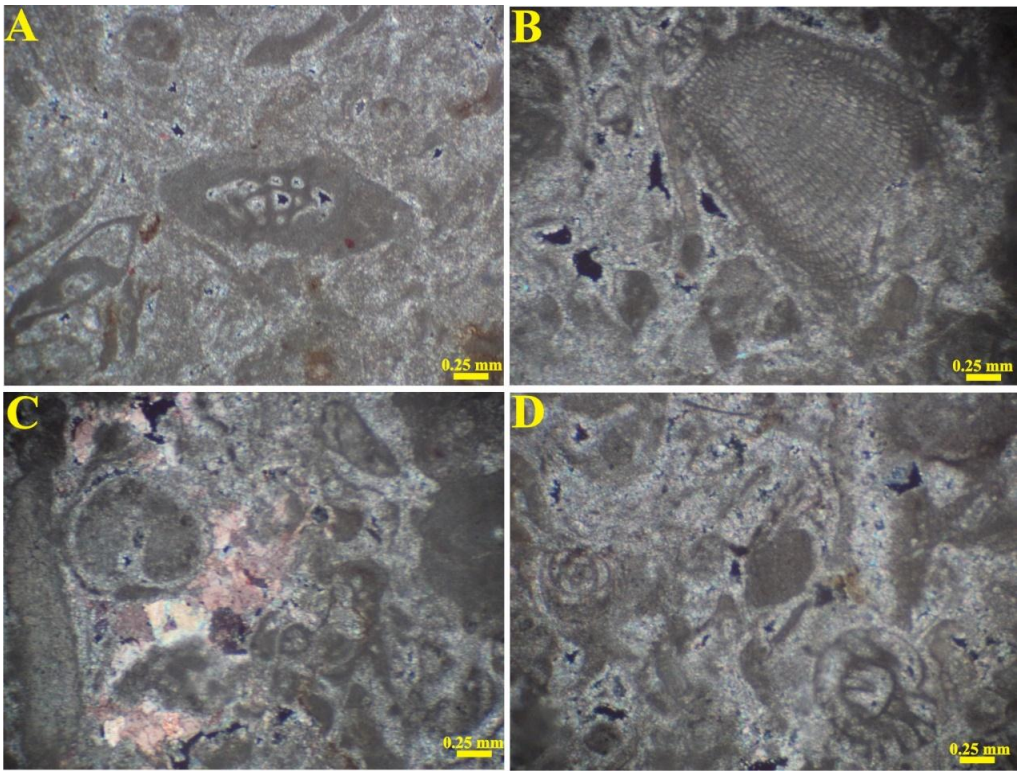

Fig.9: **A**: Benthic foraminifera/ Soritide species/ Ja12, **B**: Red algae (*Archaeolithothamnium sp.*)/ Ja9, **C**: Benthic foraminifera/ Mollusca shells/ Jb21, and **D**: Benthic foraminifera/ Milliods and peneroplis species/ Jb15

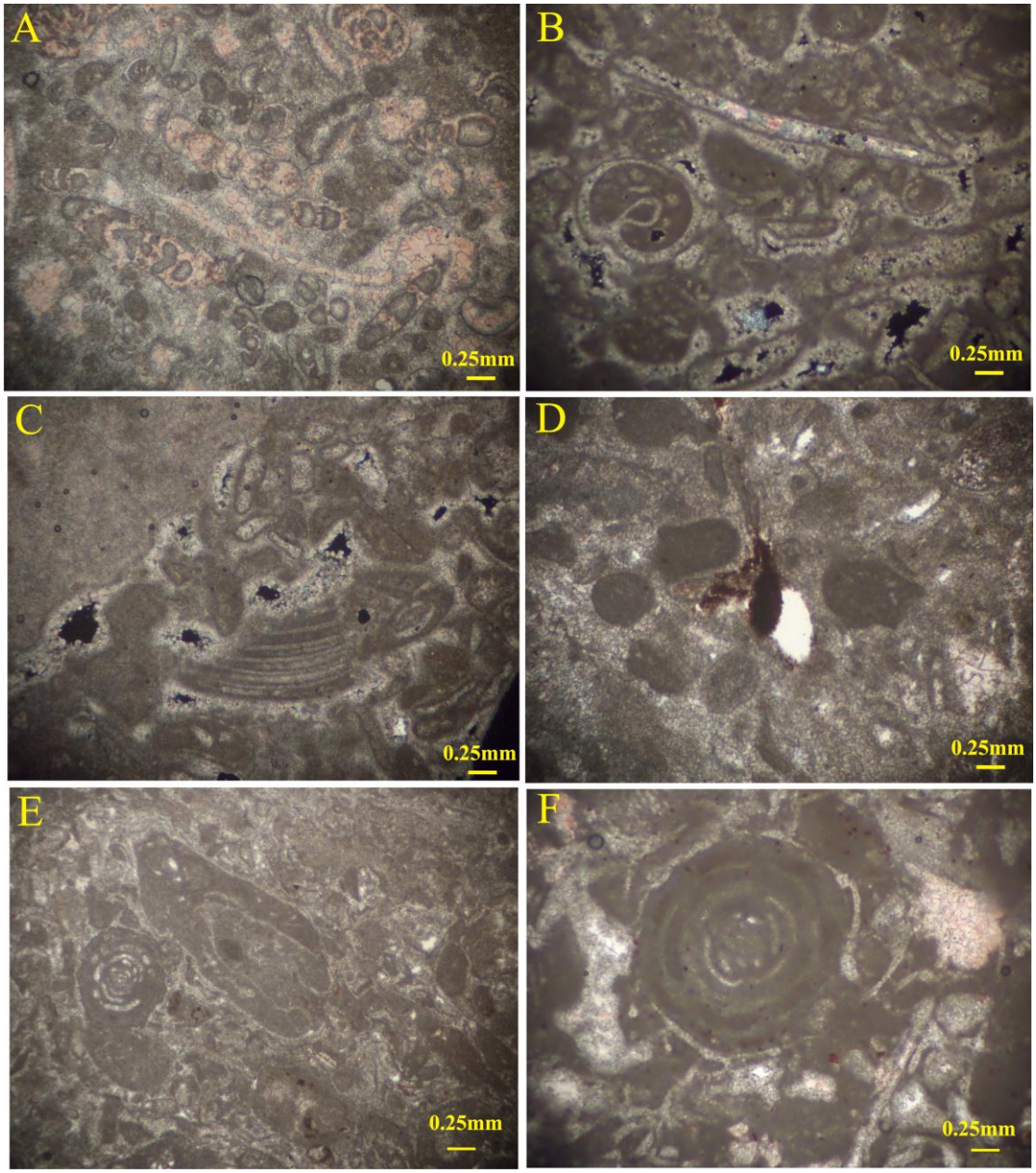

Fig.10: **A**: Abundant Gastropoda fragment, Peneroplis *sp.*, miliolids *sp* and shell fragments /Jb19, **B**: Abundant Peneroplis *sp.*, miliolids *sp.*/ Jb39, **C**: Pellets, Peneroplis *sp.*, boroles *sp* and shell fragments/ Jb31, **D**: Archais *sp.* and peneroplis *sp.*/ Jb19, and **E** and **F**: Borelis melo melo/ Ja 15 and 13

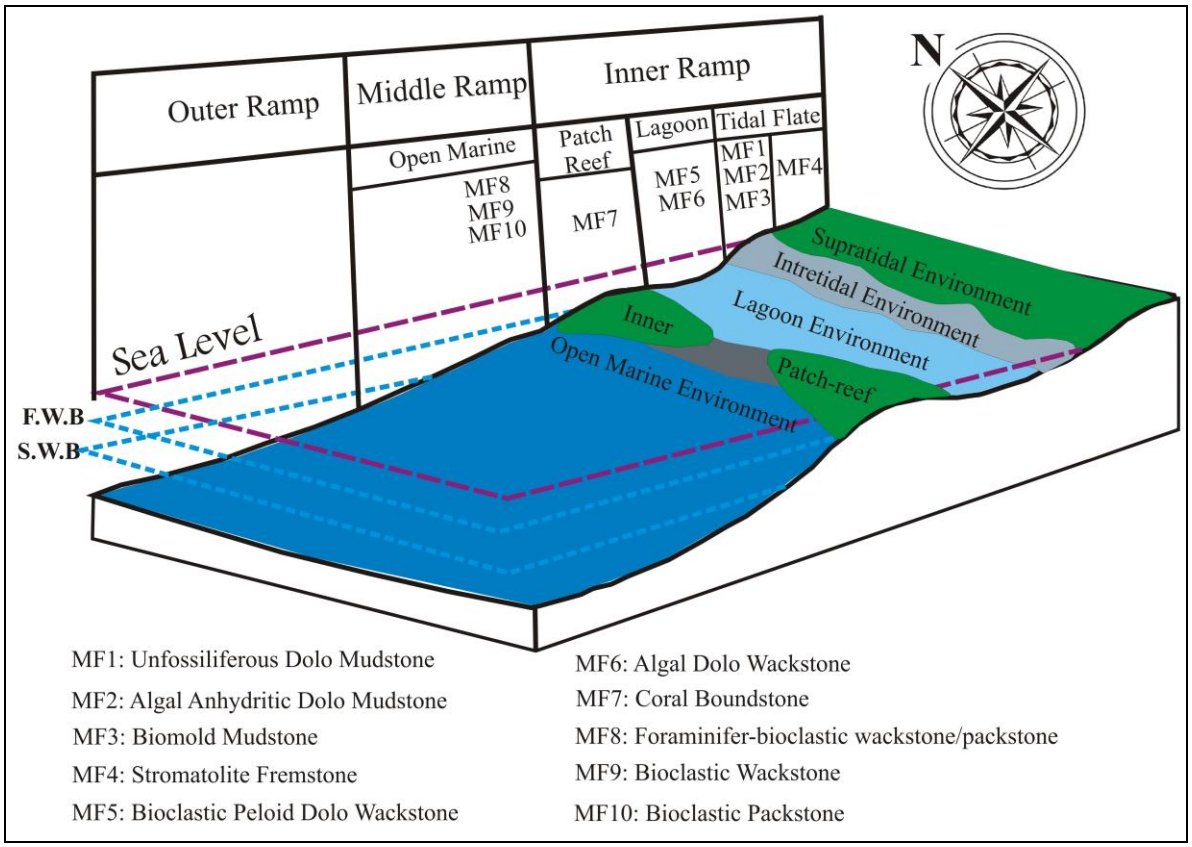

Fig.11: The proposed block diagram shows an imaginated depositional model of the Jeribe Formation in the study area

- **FA1: Tidal Flat (Supratidal and Intretidal) Facies Association**

Supratidal and Intertidal environments characterize tidal Flat. The Intertidal was observed at lower and upper contact of the Jeribe Formation with the thickness (7 and 5 m), respectively. Intertidal facies association consists of **MF1:** unfossiliferous dolo Mudstone, **MF2:** Algal anhydrite dolo mudstone, and **MF3:** biomold dolomudstone, containing scattered skeletal grains of algae (red and green algae) and biomold of benthic Foraminifera (miliolids *sp*) in places laminated, grey colored, and the groundmass consist of dolosprite, the dolomite diagenetically recrystallized medium to coarser crystals. These microfacies have been observed in the lower and upper part of the contract with underlined and overlined formations. The intertidal zone is highly inhospitable to marine organisms due to high temperatures and abnormal salinities. As a result, the highest density of biogenic structures in tropical tidal flats is found in the lower intertidal zone (Terwindt, 1988). In relatively colder areas, tidal flats may exhibit a high density of biogenic structures in the intertidal zone (Desjardins *et al*., 2012; Terwindt, 1988). This gradient from Unfossiliferous to biomold of benthic Foraminifera mudstone indicates a gradient in temperatures from very high to moderate temperatures.

Supratidal facies association consists of **MF4:** Stromatolites fremstone with a thickness of 3 m, characterized by Algal mats, which are identified as a laminated structure. The simplest type is planar or slightly undulating and has been referred to as cryptaalgal laminates (Aitken, 1967). Stromatolites or stromatoliths are defined by (Riding, 1991) "as layered accretionary structures formed in shallow water by trapping, binding and cementation of

sedimentary grains by layers of microorganisms, especially cyanobacteria (commonly known blue-green algae)". These facies correspond to SMF-23 of Wilson (1975) and Flügel (2010). The deposition setting occurred in a low-energy, restricted intertidal environment.

- **FA2: Lagoonal Facies Association (Semi-Restricted Lagoon)**

Lagoonal facies association is characterized by **MF5:** Bioclastic Peloid dolowackestone/ packstone and **MF6:** Algal dolowackstone with a thickness of about (10 m). The dominant microfacies are wackestone and packstone with the majority of micritized grains indicating a quite subtidal environment. Wackestone microfacies are interpreted as shallow marine environments and the bioclastic-packstone to grainstone microfacies are indicative of deposition in relatively high energy, normal shallow marine environments (Flügel, 2004). The ground mass is clotted texture causing the merge of Peloids to a pseudo-micritic matrix. The low diversity of bioclasts (only miliolids *sp. and* Peneroplis *sp* with rare algae) and the existence of peloids and algae in these facies indicate deposition on an inner ramp, in low energy semi-restricted shallow-subtidal environments, perhaps in a peritidal setting with a connection to the middle ramp. These microfacies have been observed in the lower part of the formation and at the contact with the overline formation. These facies correspond to SMF-10 of Wilson (1975) and Flügel (2010).

- **FA3: Inner Patch-Reef Facies Association**

The reefs consist predominantly of the framework built by corals and benthic foraminifera. Which is characterized by **MF7:** Coral Boundstone/Grainstone, which has been observed in the middle part of the formation. The diagenetic process acting in these microfacies are micritization, cementation (sparry calcite), dolomitization of anhedral, and subhedral dolomite crystals.

- **FA4: Open Marine Facies Association**

Open Marine facies association characterized by **MF8:** Foraminifer-bioclastic wackestone/ packstone, these facies showing a diverse species compared to previous facies and dominant biota are benthic foraminifers among which Miliolids are Quinquilocuilina sp; Austrotrilina sp and pyrgo sp, and Archaias (large benthic foraminifera), while Soritidae species are Peneroplis sp (Peneroplis Henson and Peneroplis farsensis). Dendritina sp. and Alveolinidae species (Borelis melo sp), with shell fragments of Mollusca (gastropod) and red algae, dolomicritic matrix with fine dolomite crystals. The foraminiferal assemblages vary throughout the successions, they are dominants in open marine facies. The association of red algae and larger benthic foraminifera are known to inhabit the Oligo-photic zone of the middle ramp environment (Hoseinzadeh *et al*., 2015). All benthonic foraminifers' range between 0.1 and 0.5 mm. The study indicates the formation have been deposited in a marine environment ranging from shallow, moderate energy to relatively deeper, high-energy waters. the uncommon benthic form and dominance of red algae reflect the climatic variation and/ or upwelling current.

MF9: Bioclastic wackestone, these facies consist of abundant gastropoda fragments, Peneroplis *sp.* and Miliolids *sp*. with rare pellets and the groundmass is micrite matrix. Fragmentation of bioclasts is due to reworking in a relatively shallow-water environment by wave or tidal processes and/or from extensive bioturbation. The main characteristics of this environment are deposition in normal-marine, moderate to high energy that is not subjected to significant restriction in water circulation. **MF10:** Bioclastic packstone, these facies has been observed in the middle part, with a thickness of about (3 m). The skeletal grains comprise mainly calcareous red algae. Coralline algae (red algae) is belonging to the family

Corallianceae of the order corallinales. These are euphotic zone with shallow water depth and may extend from Lagoon to the shelf break (Amine and Thanon, 2005). Red algae do not show a distinct facies gradient in the studied samples, they are recorded in all the facies with significantly high dominance in open marine facies. Corallinacea red algae are distinguished as Autochthonous red algae and are considered the major type in the middle part of the Jeribe Formation associated with benthic foraminifers, species recognized are (*Archaeolithothamnium* and *Mesophyllum*). These microfacies have been observed in the middle part of the formation. These facies correspond to SMF-8 of Wilson (1975) and Flügel (2010).

CARBON-13 AND OXYGEN-18

Oxygen-18 data of the Jeribe Formation reflect several enrichment events that occurred during the middle Miocene age. Amplitude changes refer to two main zones of the enrichment after, which they get a lighter isotope. The values fluctuate between (1.62) to (2.89) in the lower part and (1.3) to (2.78) in the upper part with interval depletion to -0.97‰ values. The onset of Monterey excursion by sizable values CM1 (carbon maxima) 2.74‰, which are maximum enriched value, followed by a decline to a minimum positive value (0.05‰). Depletion values are in the middle parts causing discontinuous Monterey excursion disputes globally (Table 2).

Table 2: Analytical results of the $\delta^{18}O$ and the $\delta^{13}C$

Sample No.	$^{13}C_{V\text{-}PDB}$ (‰)	$^{18}O_{V\text{-}PDB}$ (‰)	Sample	$^{13}C_{V\text{-}PDB}$ (‰)	$^{18}O_{V\text{-}PDB}$ (‰)
JA21	1.30	1.23	JB9	2.74	2.67
17JA	0.71	1.18	JB11	-0.45	1.49
5JA1	-0.14	1.17	JB15	2.14	1.50
3JA1	1.01	1.21	JB17	2.26	2.66
1JA1	1.80	1.47	JB21	2.37	2.78
JA10	-0.87	0.12	JB27	2.14	1.75
JA9	1.07	1.62	JB31	1.65	0.99
JA6	1.59	2.80	JB37	1.31	1.22
1JA	-1.07	-0.97	JB39	0.05	0.45
JB7	2.44	2.89	JB42	-1.14	-1.15

DISCUSSION

The primary isotopic signatures are readily altered during the diagenetic processes of the skeletal and non-skeletal components of the carbonate sediments (Armstrong-Altrin *et al*., 2011). Multiple methods have been developed to assess $\delta^{18}O$ and $\delta^{13}C$ variations during diagenetic influences involving correlation between $\delta^{18}O$ and $\delta^{13}C$ (Ali and Sa'ad, 2018; Armstrong-Altrin *et al*., 2011; Oehlert and Swart, 2014). The $\delta^{18}O$ isotope is more prone to diagenetic overprint and highly sensitive to temperature changes, especially in the bulk carbonate (Schobben *et al*., 2016). Therefore, a positive correlation between $\delta^{18}O$ and $\delta^{13}C$ reflects primary marine isotopic signals. As shown in Figure 12, the stable isotopes result of the Jeribe Formation is displaying a strong correlation between $\delta^{13}C$ and $\delta^{18}O$ ($r = 0.85$). Generally, it refers to the lack of significant influence of diagenesis on the stable isotopic composition. Bivariate plots of $\delta^{18}O$ and $\delta^{13}C$ are another convenient method. It is used to distinguish the depositional and/ or diagenetic environments of carbonate rocks.

(Hudson 1977; Nelson and Smith 1996) had used a $\delta^{18}O$ and $\delta^{13}C$ cross-plot to identify the origins of different types of carbonate rocks. Therefore, this approach has been adopted by many workers, such as (Bathurst 1983; Choquette and James 1987; Moore 1989; Morse and Mackenzie 1990). Despite significant effaces of evaporation, meteoric dilution, and carbon transfer in the shallow marine relative to platform margin, slope, and basinal environments, the isotopes composition in the investigated succession exhibits primary stable isotope values and can be used as a direct proxy for the composition of seawater in the Kirkuk-Dezful Embayment during the Middle Miocene (Figure 13).

Carbonates of the Jeribe Formation show vertical variation in $\delta^{18}O$ and $\delta^{13}C$ composition; however, most samples have positive values. At the contact of the succession, the boundary of the Early-Middle Miocene and Middle-late Miocene are marked by prominent negative values of the $\delta^{18}O$ and $\delta^{13}C$. It is clearly expressed by a vertical change in the environmental conditions from the lagoon to the distal ramp, patch reef environment, and inner ramp facies in the uppermost at the contact with the overlying and underlying formations. However, both isotopes ($\delta^{18}O$ and $\delta^{13}C$) display enrichment after depletion, which is marking the beginning of transgression in the Middle Miocene, denoting the Ng30 date of the final closure of Neo-Tethys by Sharland *et al*. (2004). Enrichment of both $\delta^{13}C$ and $\delta^{18}O$ isotopes has occurred in two main zones, Mio2 and Mio3. It is separated by relatively depleted in the middle unit, on both the $\delta^{13}C$ and $\delta^{18}O$ (Figure 8).

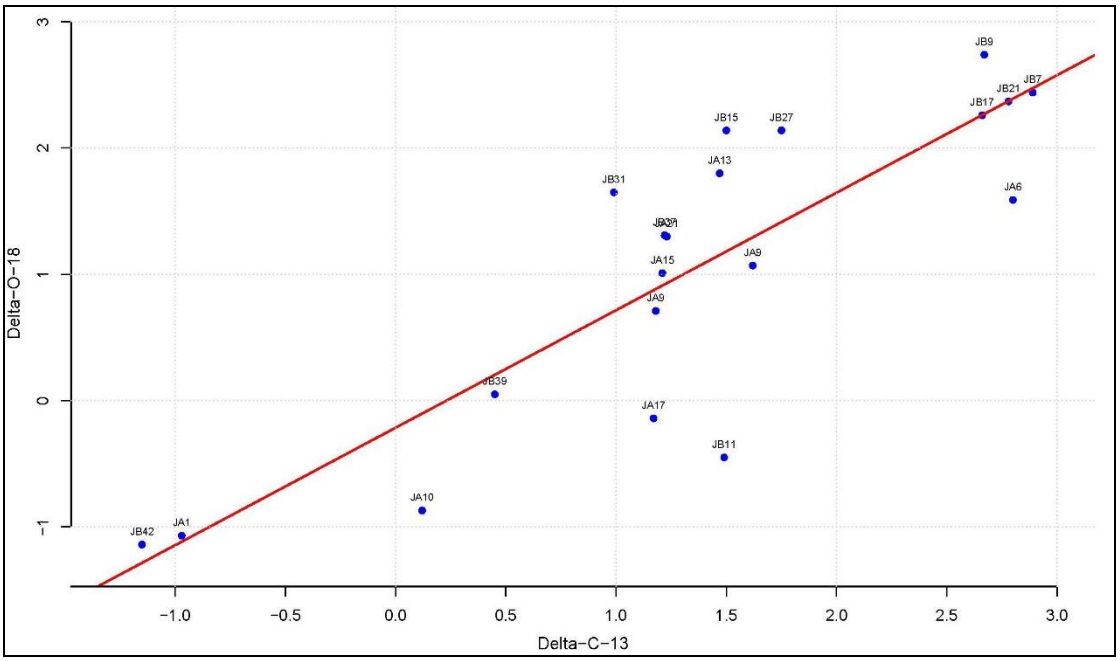

Fig.12: Correlation between the $\delta^{13}C$ and the $\delta^{18}O$

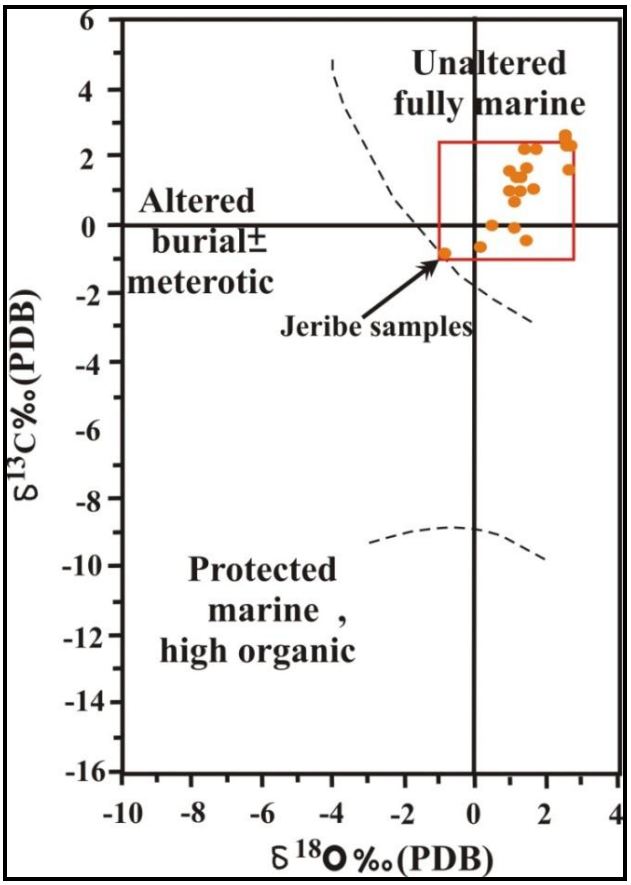

Fig.13: $\delta_{18}O$ and $\delta_{13}C$ plots from the Jeribe Formation showing the primary signature of isotopes

Mi zones have been identified and defined using the criteria of Miller *et al*. (1991) based on the maximum $\delta^{18}O$ value. The current study represents a single global point recorded with more details about Mi2 and Mi3 zones, where Mi3 has been subdivided into Mi2b, Mi2c, and Mi2d, while Mi3 zone is subdivided into Mi3a, Mi3b, and Mi3c. These discernible deviations represent a minor step in the major cooling trend that started with Mi 3 and Mi2, that gradual increase in glaciation has a profound and immediate impact on the depositional environment of the Jeribe Formation. expressed by transit from the lagoon and patch reef to the open marine environment.

Coralline algae are used to assess the paleo-climate, paleo-latitudes, and paleo-depth (Sophie and Kamenos, 2015). They have a wide temperature range tolerate and live at depths of 125 m or more in moderate wave energy areas (Scholle and Ulmer-Scholle, 2003). They are sensitive to water depth and terrigenous input. Corallines, in general, prefer decreased siliciclastic loading and shallow to mildly deeper bathymetry (Sarkar *et al*., 2016). Coralline red algae of the corallinales order (Archaeolithothamnium sp. and Mesophyllum sp.) are identified as autochthonous forms. They comprise the major type of open marine environment of the Jeribe Formation associated with coral and benthic foraminifera in the lagoon and patch reef environments.

Dasycladaceae is one of the large calcareous green algae families, which are not abundant in the Jeribe Formation. The green and red algae are observed in the onset of the lower unit of the studied sections. Dasycladaceae green algae commonly occur in quiet, shallow, or very

shallow, normal salinity, and warm water in the reef-lagoon environment (Flügel, 2004). This environment is characterized by abundant green algae at depths of 50 – 100 m in the reef and tidal flat areas. It is more significant in modern and ancient carbonate deposits of warm water regions (Scholle and Ulmer-Scholle, 2003). Green algae are mostly indicative of back reef-lagoon facies and/ or the lower zone of the intertidal setting. The distribution of small encrusting green and red algae can be used to estimate the depth-related zones and climate (Flügel, 2012).

The presence of red and green algae together indicates that the sedimentation had occurred in the upper part of the photic zone (Flügel, 2012). The absence of green algae in the lower part within the lagoonal environments and the middle part within the coral patch-reef facies reflect cold water relatively; while the uppermost part within the intertidal facies reflects high energy.

The recognized coral occurs in the middle part of the successions. It represents tropical environments, normal salinity, and waters at depths from the intertidal zone to a few tens of meters. It is mainly in areas with a relatively low influx of terrigenous sediments (Scholle and Ulmer-Scholle, 2003). Corals contributed significantly to the formation of large and extended reef structures in deeper- and cold-water settings. However, it is also in relatively shallow warm-temperate environments (Flügel, 2004). Corals that occur in situ were found in a shelf sequence formed during a relatively sea-level highstand (Scholle and Ulmer-Scholle, 2003). Observed coral reefs and the absence of green algae indicated sea level rise (Flügel, 2004).

In the upper part, red algae, stromatolites, and benthic foraminifera are identified. Corallinacean algae and abundant foraminiferal types reflect the shallow open marine environments (Flügel, 2012). Red algae and the benthic foraminifera emphasize deposition in the upper photic zone to the upper part of the lower photic zone (Flügel, 2010). Stromatolites were observed in the upper part of the succession within supratidal/ sabkha environments. It represents the range from subtidal to intertidal settings (Scholle and Ulmer-Scholle, 2003). They are commonly set in tidal and subtidal carbonates as well as in subtidal shelf carbonates or shallow subtidal environments. They take their energy from the decomposition of organic material to inorganic components by redox processes in shallow-water settings (Flügel, 2004).

The variation of oxygen and carbon isotope composition in response to dynamic seawater underwent a dramatic change in depositional facies. In the intertidal environments, mudstone facies exhibit the lowest values on both $\delta^{13}C$ and $\delta^{18}O$, while in the lagoonal environments/ wackestone facies display shifts towards high values. $\delta^{18}O$ reflects a combined effect of temperature and ice-volume formation (Zachos *et al*., 2001). Therefore, intense fluctuations in global sea level are caused by glacioeustasy. During glacial times, the ocean waters become heavier O than during interglacial times (Bradley, 1999). (CM1) event formed over wackestone facies within lagoon environments, that occurrences as the interval between two major cooling Mi2a and Mi2b. Enrichment by $\delta^{18}O$ and absences of green algae are indicative of glacial climate, suggesting the differentiation between the mudstone and wackestone facies and their skeletal grains from laminated algae with some pellets to red algae and milliods sp. due to different depositional energy, which appears to be the major controlling factor to the heaviest and linked to glacioeustasy. Suggests minor steps of interglacial events and relative sea level rise. In the open marine environment, moderate energy represents by wackestone and packstone facies exhibit the highest values of ^{13}C and formed (CM 2), associated with a minor step in the major cooling. Glacio-eustatic sea-level rose has been controlling facies change and indicates an upwelling current.

High energy in grainstone facies within the patch-reef environments display depleted on both $\delta^{13}C$ and $\delta^{18}O$ marked interglacial events separate major glacial zones Mi2 and Mi3. Coral reefs are important proxy data due to their temperature sensitivity. It's affected by cooling episodes that prevented coral reef growth. This shift to depletion allowed for predictive short-term inter-glacial events. According to Immenhauser *et al.* (2002), restricted-platform water displays relatively low ^{13}C values due to remineralized organic carbon during the long residence time of seawater on the platform.

The low $\delta^{13}C$ values are translated into the shallow-water carbonate platforms tend to become an influence on meteoric water during sea-level fall. According to (Purkis *et al*., 2015), grainstone and boundstone facies are indicative of water depths < 5 m. Sea level underwent fall in this interval is caused by glacial events.

Open marine facies showed substantial variation in the $\delta^{13}C$ and $\delta^{18}O$ associated with a change in skeletal grain. Open marine environments represent by wack-packstone and packstone facies with significant differences in the types of the skeletal grain to red algae and benthic foraminifera (Miliolids, Soritidae, and Alveolinidae species, with Mollusc shells) displaying the highest values on both the $\delta^{13}C$ and $\delta^{18}O$ and formed CM3 to 6 events, synchronous with major glacial zones Mi3a, b, and c. Shifted to depletion on the ^{13}C and ^{18}O value at the onset of the supratidal/sabkha facies with significant differences in the types of the skeletal grain to Domal Stromatolite, Densely laminated compared to other fossils. These events match with short-term event records indicated by depletion in ^{18}O relatively near 0‰ and display the more negative value in ^{13}C as interval events between CM5 and 6, suggesting interglacial periods as a minor step of major cooling. High energy in the packstone facies of the intertidal environments at the upper contact displays more negative on both ^{13}C and ^{18}O values. Shoaling reflects climatic and oceanographic changes that impacted the integral closure of the Tethys seaway during the middle Miocene.

On these bases, the variability of ^{13}C came from depositional energy in the shallowest setting that linked to glacial-eustatic within Mi2 and Mio3 zones. Decreases in the $\delta^{13}C$ values reflect variations in carbonate production and accumulation rates because the carbonate production is lower in the cool water, Interglacial periods are indicated coincidentally with high carbonate production. According to Grossman (2008), sea level falls, as continental ice sheets and glaciers expand is a primary force that influences.

According to Mason *et al*. (2017), carbon originated from the volcanic arc and represents an essential source in the marine environment. Subduction-related volcanic arcs, particularly, continental arcs, are the main source of heavier carbon due to the reworking of crustal limestone that is often associated with the closing of ocean basins. Weissert and Erba (2004) mentioned that the major positive C-isotope anomalies in the Early Cretaceous coincide with episodes of volcanic activity. Moreover, the volcanic arc that occurred during the thrusting and later closing of the ocean is combined with increased ^{13}C, suggesting a high $\delta^{13}C$ concentration as CM-events in shallow marine carbonates linked to the structural location of Kirkuk-Dezful Embayment, which is lying adjacent to the volcanic activity and coincide to the platform destruction during the final phase of Tethys Sea closure. Many published papers mentioned that Mi 3b is marking the final major cooling step and the end of the Monterey Excursion (Miller *et al*. 1991; Shevenell *et al*., 2004 and 2008; Zachos *et al*., 2001; Zachos *et al*., 2008). In the current details study, Mi 3c marking the final major cooling coincide with the end of the Monterey Excursion (Figure 14).

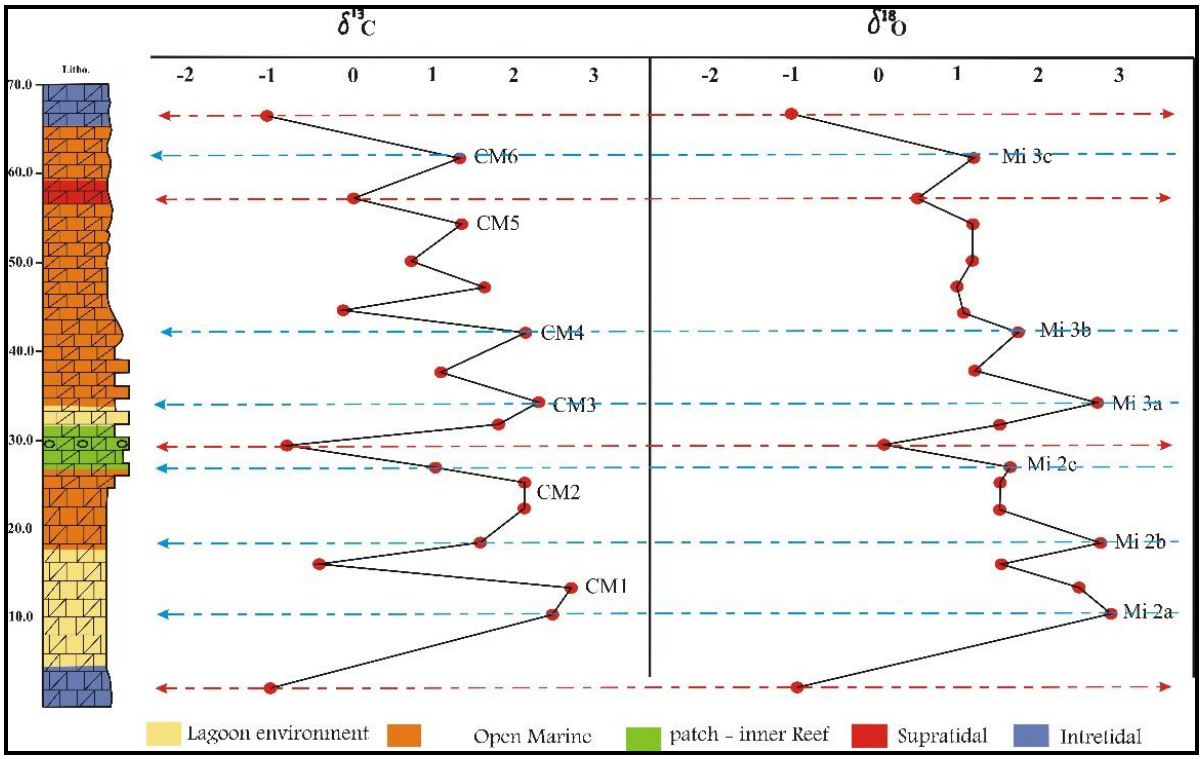

Fig.14: Stable isotope distribution in the Jeribe succession

CONCLUSIONS

This study focused on identifying the facies of the Jeribe Formation and stable isotopes. This formation is deposited during the final phase of the Tethys Sea closure (Middle Miocene age) as a shallow marine deposition on the Arabian plate.

Mi zones have been identified based on the maximum $\delta^{18}O$ value. Middle Miocene in the shallowest marine has Mi2, Mi3, and Mi 3a zones with additional details about Mi2 and Mi3 zones. The Mi3 has a minor step in the significant cooling represented by Mi3a, Mi3b, and Mi3c. Mi2 zone is also subdivided into three minor steps: Mi2a, Mi2b, and Mi2c. These deviations denote Mi zones represent cool water by increasing upwelling current and prominent facies changes occur synchronously with CM-event, subsequently with high sedimentation rates. The positive value of the ^{13}C (CM-events) is controlled by proximity to the depositional energy and tectonic activities, which can bury carbonate-producing organisms and enhance ^{13}C. The peaks of heavy ^{13}C represent polyphase deformation and platform destruction in the subduction zone on the northeastern margin of the Arabian plate.

ACKNOWLEDGMENTS

The authors would like to express their sincere thanks and appreciation to Dr. Ibrahim Q. Mohammed and Sahira Karim for their unlimited logistic assistance and their valuable work, field information, and comments significantly improved the manuscript with valuable comments.

REFERENCES

Aitken, James D. 1967. Classification and Environmental Significance of Cryptalgal Limestones and Dolomites, with Illustrations from the Cambrian and Ordovician of Southwestern Alberta. Journal of Sedimentary Research, Vol.37, No.4, p. 78 – 1163.

Ali, Mustafa, A. and Sa'ad., Z., 2018. Application of 18O And 13C Stable Isotopes Composition of the Carbonate Rocks of the Jeribe Formation Eastern Iraq; An Approach to Define the Paleo Temperature and Paleo Depth. The Iraqi Geological Journal, p. 83 – 100.

Amodio, S., Ferreri,V., D'Argenio, B., Weissert, H. and Sprovieri., M., 2008. Carbon-Isotope Stratigraphy and Cyclostratigraphy of Shallow-Marine Carbonates: The Case of San Lorenzello, Lower Cretaceous of Southern Italy. Cretaceous Research, Vol.29, No.5 – 6, p. 13 – 803. DOI: 10.1016/j.cretres.2008.05.022.

Aqrawi, A.A.M., Mahdi, T.A., Sherwani, G.H. and Horbury, A.D., 2010. Characterization of the Mid-Cretaceous Mishrif Reservoir of the Southern Mesopotamian Basin, Iraq. p. 7 – 10 in American Association of Petroleum Geologists Conference and Exhibition. Vol.7.

Armstrong-Altrin, J.S., Lee, Y.I., Verma, S.P. and Worden, R.H., 2009. Carbon, Oxygen, and Strontium Isotope Geochemistry of Carbonate Rocks of the Upper Miocene Kudankulam Formation, Southern India: Implications for Paleoenvironment and Diagenesis. Chemie Der Erde, Vol.69, No.1, p. 45 – 60. doi: 10.1016/j.chemer.2008.09.002.

Armstrong-Altrin, John S., J. Madhavaraju, Alcides N. Sial, Juan J. Kasper-Zubillaga, R. Nagarajan, K. Flores-Castro, and Janet Luna Rodríguez. 2011. Petrography and Stable Isotope Geochemistry of the Cretaceous El Abra Limestones (Actopan), Mexico: Implication on Diagenesis. Journal of the Geological Society of India, Vol.77, No.4, p. 59 – 349.

Auer, G., Piller, W.E., Reuter, M. and Harzhauser, M., 2015. Correlating Carbon and Oxygen Isotope Events in Early to Middle Miocene Shallow Marine Carbonates in the Mediterranean Region Using Orbitally Tuned Chemostratigraphy and Lithostratigraphy. Paleoceanography, Vol.30, No.4, p. 52 – 332. doi: 10.1002/2014PA002716.

Bathurst, R.G.C., 1983. Early Diagenesis of Carbonate Sediments. p. 349 – 77 in Sediment Diagenesis. Springer.

Bellen, R.C. Van, H.V Dunnington, Rm Wetzel, and D. Morton. 1959. Lexique Stratigraphic International. Asie, Fasc. 10a, Iraq, Paris, 333pp.

Billups, K. and Schrag, D.P., 2003. Application of Benthic Foraminiferal Mg/Ca Ratios to Questions of Cenozoic Climate Change. Earth and Planetary Science Letters, Vol.209, No. 1 – 2, p. 95 – 181.

Bradley, Raymond, S., 1999. Paleoclimatology: Reconstructing Climates of the Quaternary. Elsevier.

Chakrabarti, Gopal, Debasish Shome, Subhasish Kumar, John S. Armstrong-Altrin, and Alcides N. Sial. 2011. Carbon and Oxygen Isotopic Variations in Stromatolitic Dolomites of Palaeoproterozoic Vempalle Formation, Cuddapah Basin, India. Carbonates and Evaporites, Vol.26, No.2, p. 91 – 181.

Chaproniere, George, C.H., 1981. Late Oligocene to Early Miocene Planktic Foraminiferida from Ashmore Reef No. 1 Well, Northwest Australia. Alcheringa, Vol.5, No.2, p. 31 – 103.

Choquette, Philip W., and Noel P. James. 1987. Diagenesis# 12. Diagenesis in Limestones-3. The Deep Burial Environment. Geoscience Canada.

Cooke, Penelope J., Campbell S. Nelson, and Martin P. Crundwell. 2008. Miocene Isotope Zones, Paleotemperatures, and Carbon Maxima Events at Intermediate Water- depth, Site 593, Southwest Pacific. New Zealand Journal of Geology and Geophysics, Vol.51, No.1, p. 1 – 22.

Coplen, Tyler B., Carol Kendall, and Jessica Hopple. 1983. Comparison of Stable Isotope Reference Samples. Nature, Vol.302, No.5905, p. 38 – 236.

Corfield, R.M. and Cartlidge, J.E., 1993. Oxygen and Carbon Isotope Stratigraphy of the Middle Miocene, Holes 805B and 806B. in Proceedings of the Ocean Drilling Program. Scientific Results. Vol.130, p. 307 – 22.

Desjardins, Patricio, R., Luis, A. Buatois, and M. Gabriela, Mangano, 2012. Tidal Flats and Subtidal Sand Bodies. Developments in Sedimentology, Vol.64, p. 61 – 529.

Diester- Haass, Liselotte, Katharina Billups, Ingrid Jacquemin, Kay C. Emeis, Vincent Lefebvre, and Louis François, 2013. Paleoproductivity during the Middle Miocene Carbon Isotope Events: A Data- model Approach. Paleoceanography, Vol.28, No.2, p. 46 – 334.

Edgar, Kirsty M., Eleni Anagnostou, Paul N. Pearson, and Gavin L. Foster. 2015. Assessing the Impact of Diagenesis on Δ11B, Δ13C, Δ18O, Sr/Ca and B/Ca Values in Fossil Planktic Foraminiferal Calcite. Geochimica et Cosmochimica Acta, Vol.166, p. 189 – 209.

Flower, B.P. and Kennett, J.P., 1993. Relations between Monterey Formation Deposition and Middle Miocene Global Cooling: Naples Beach Section, California. Geology, Vol.21, No.10, p. 877 – 80. doi: 10.1130/0091-7613(1993)021<0877:RBMFDA>2.3.CO;2.

Flower, Benjamin P. and James P. Kennett, 1994. The Middle Miocene Climatic Transition: East Antarctic Ice Sheet Development, Deep Ocean Circulation, and Global Carbon Cycling. Paleogeography, Palaeoclimatology, Palaeoecology, Vol.108, No. 3 – 4, p. 55 – 537.

Flower, Benjamin P., and James P. Kennett, 1995. Middle Miocene Deepwater Paleoceanography in the Southwest Pacific: Relations with East Antarctic Ice Sheet Development. Paleoceanography, Vol.10, No.6, p.1095 – 1112.

Flügel, Erik, 2012. Microfacies Analysis of Limestones. Springer Science and Business Media.

Flügel, Erik, and Erik Flügel, 2004. Microfacies of Carbonate Rocks: Analysis, Interpretation, and Application. Springer Science and Business Media.

Fouad, Saffa, F.A., 2012. Western Zagros Fold-Thrust Belt, Part I: The Low Folded Zone. Iraqi Bull. Geol. Min. Vol.5, p. 39 – 62.

Flügel, E. and Munnecke, A., 2010. Microfacies of carbonate rocks: analysis, interpretation and application, Berlin: springer, Vol.976, 2004pp.

Gröcke, Darren R., Gregory D. Price, Stuart A. Robinson, Evgenij Y. Baraboshkin, Jörg Mutterlose, and Alastair H. Ruffell, 2005. The Upper Valanginian (Early Cretaceous) Positive Carbon–Isotope Event Recorded in Terrestrial Plants. Earth and Planetary Science Letters, Vol.240, No.2, p. 495 – 509.

Grossman, Eric E. 2008. Sea Level and Its Effects on Reefs in Hawai'i. U.S. Geological Survey Scientific Investigations Report, 2007-5101, p. 101– 4.

Holbourn, Ann, Wolfgang Kuhnt, Michael Schulz, J.A. José-Abel Flores, and Nils Andersen, 2007. Orbitally-Paced Climate Evolution during the Middle Miocene 'Monterey' Carbon-Isotope Excursion. Earth and Planetary Science Letters, Vol.261, No.3 – 4, p. 50 – 534. doi: 10.1016/j.epsl.2007.07.026.

Hudson, J.D., 1977. Stable Isotopes and Limestone Lithification. Journal of the Geological Society, Vol.133, No.6, p. 60 – 637.

Hoseinzadeh, M., Daneshian, J., Moallemi, S.A. and Solgi, A., 2015. Facies analysis and depositional environment of the Oligocene-Miocene Asmari Formation, Bandar abbas hinterland, Iran. Open Journal of Geology, Vol.5, No.04, 175pp.

Immenhauser, Adrian, Jeroen A. M. Kenter, Gerald Ganssen, Juan R. Bahamonde, Arjan Van Vliet, and Margot H. Saher, 2002. Origin and Significance of Isotope Shifts in Pennsylvanian Carbonates (Asturias, NW Spain). Journal of Sedimentary Research, Vol.72, No.1, p. 82 – 94.

Jassim, S.Z. and Goff, J.C., 2006. Geology of Iraq. Dolin, Prague and Moravian Museum. Brno, 341pp.

Kumar, B., S. Das Sharma, B. Sreenivas, A. M. Dayal, M. N. Rao, N. Dubey, and B. R. Chawla. 2002. Carbon, Oxygen and Strontium Isotope Geochemistry of Proterozoic Carbonate Rocks of the Vindhyan Basin, Central India. Precambrian Research, Vol.113, No. 1 – 2, p. 43 – 63.

Madhavaraju, J., Kolosov, I., Buhlak, D., Armstrong-Altrin, J.S., Ramasamy, S. and Mohan, S.P., 2004. Carbon and Oxygen Isotopic Signatures in Albian-Danian Limestones of Cauvery Basin, Southeastern India. Gondwana Research, Vol.7, No.2, p. 29 – 519.

Maheshwari, Anil, A.N. Sial, Rajeeva Guhey, and V.P. Ferreira, 2005. C-Isotope Composition of Carbonates from Indravati Basin, India: Implications for Regional Stratigraphic Correlation. Gondwana Research, Vol.8, No.4, p. 10 – 603.

Marquillas, R., Sabino, I., Nobrega Sial, A., Papa, C.d., Ferreira, V. and Matthews, S., 2007. Carbon and Oxygen Isotopes of Maastrichtian-Danian Shallow Marine Carbonates: Yacoraite Formation, Northwestern Argentina. Journal of South American Earth Sciences, Vol.23, No.4, p. 20 – 304. doi: 10.1016/j.jsames.2007.02.009.

Mason, Emily, Marie Edmonds, and Alexandra V. Turchyn, 2017. Remobilization of Crustal Carbon May Dominate Volcanic Arc Emissions. Science, Vol.357, No.6348, p. 94 – 290.

Miller, Kenneth G., Mark D. Feigenson, James D. Wright, and Bradford M. Clement, 1991. Miocene Isotope Reference Section, Deep Sea Drilling Project Site 608: An Evaluation of Isotope and Biostratigraphic Resolution. Paleoceanography, Vol.6, No.1, p. 33 – 52.

Miller, Kenneth, G. and Miriam, E. Katz, 1987. Oligocene to Miocene Benthic Foraminiferal and Abyssal Circulation Changes in the North Atlantic. Micropaleontology, Vol.33, No.2, p. 97 – 149.

Miller, Kenneth G., James D. Wright, and Richard G. Fairbanks. 1991. Unlocking the Ice House: Oligocene- Miocene Oxygen Isotopes, Eustasy, and Margin Erosion. Journal of Geophysical Research: Solid Earth, Vol.96, No.B4, p. 48 – 6829.

Moore, Clyde H., 1989. Carbonate Diagenesis and Porosity. Elsevier.

Morse, John W. and Fred T. Mackenzie, 1990. Geochemistry of Sedimentary Carbonates. Elsevier.

Mourik, A.A., Bijkerk, J.F., Cascella, A., Hüsing, S.K., Hilgen, F.J., Lourens, L.J. and Turco, E., 2010. Astronomical Tuning of the La Vedova High Cliff Section (Ancona, Italy) – Implications of the Middle Miocene Climate Transition for Mediterranean Sapropel Formation. Earth and Planetary Science Letters, Vol.297, No. 1 – 2, p. 249 – 61.

Amine, A., Mumtaz and Thanon, A., Thanon, 2005. Microfacies and paleoenvironment of Sinjar Formation (Paleocene Early Eocene), Sinjar area, northern Iraq. Raf Jour. Sci., geological special Issue, Vol.16, No.1, p. 1 – 20.

Nagarajan, Ramasamy, Alcides N. Sial, John S. Armstrong-Altrin, Jayagopal Madhavaraju, and Raghavendra Nagendra, 2008. Carbon and Oxygen Isotope Geochemistry of Neoproterozoic Limestones of the Shahabad Formation, Bhima Basin, Karnataka, Southern India. Revista Mexicana de Ciencias Geológicas, Vol.25, No.2, p. 35 – 225.

Nelson, Campbell S. and Abigail M. Smith, 1996. Stable Oxygen and Carbon Isotope Compositional Fields for Skeletal and Diagenetic Components in New Zealand Cenozoic Nontropical Carbonate Sediments and Limestones: A Synthesis and Review. New Zealand Journal of Geology and Geophysics, Vol.39, No.1, p. 93 – 107. DOI: 10.1080/00288306.1996.9514697.

Numan, Nazar. 1997. A Plate Tectonic Scenario for the Phanerozoic Succession in Iraq. Iraqi Geological Journal, Vol.30, p. 85 – 119.

Oehlert, Amanda M., and Peter K. Swart, 2014. Interpreting Carbonate and Organic Carbon Isotope Covariance in the Sedimentary Record. Nature Communications, Vol.5, No.1, p. 1 – 7.

Purkis, Sam J., Gwilym P. Rowlands, and Jeremy M. Kerr. 2015. Unraveling the Influence of Water Depth and Wave Energy on the Facies Diversity of Shelf Carbonates. Sedimentology, Vol.62, No.2, p. 541 – 65.

Raymo, Maureen E., William F. Ruddiman and Philip N. Froelich, 1988. Influence of Late Cenozoic Mountain Building on Ocean Geochemical Cycles. Geology, Vol.16, No.7, p. 53 – 649.

Rea, D. K., I. Snoeckx, and L. H. Joseph, 1998. Late Cenozoic Eolian Deposition in the North Pacific: Asian Drying, Tibetan Uplift, and Cooling of the Northern Hemisphere. Paleoceanography, Vol.13, No.3, p. 24 – 215. doi: 10.1029/98PA00123.

Riding, Robert 1991. Classification of Microbial Carbonates. In *Calcareous algae and stromatolites*. Springer, p. 21 – 51.

Ruddiman, William F., Maureen E. Raymo, Warren L. Prell, and John E. Kutzbach, 1997. The Uplift-Climate Connection: A Synthesis. In Tectonic uplift and climate change. Springer, p. 471 – 515

Sarkar, Suman, Amit K. Ghosh, and G. M. Narasimha Rao. 2016. Coralline Algae and Benthic Foraminifera from the Long Formation (Middle Miocene) of the Little Andaman Island, India: Biofacies Analysis, Systematics, and Palaeoenvironmental Implications. Journal of the Geological Society of India, Vol.87, No.1, p. 69 – 84.

Sophie J. McCoy and Kamenos Nicholas, A., 2015. Coralline algae (Rhodophyta) in a changing world: Integrating ecological, physiological, and geochemical responses to global change, Phycology published by Wiley Periodicals, Vol.51, p. 6 – 24. DOI: 10.1111/jpy.12262

Schobben, Martin, Clemens Vinzenz Ullmann, Lucyna Leda, Dieter Korn, Ulrich Struck, Wolf Uwe Reimold, Abbas Ghaderi, Thomas J. Algeo, and Christoph Korte, 2016. Discerning Primary versus Diagenetic Signals in Carbonate Carbon and Oxygen Isotope Records: An Example from the Permian – Triassic Boundary of Iran. Chemical Geology, Vol.422, p. 94 – 107.

Scholle, Peter A. and Michael A. Arthur. 1980. Carbon Isotope Fluctuations in Cretaceous Pelagic Limestones: Potential Stratigraphic and Petroleum Exploration Tool. Aapg Bulletin, Vol.64, No.1, p. 67 – 87.

Scholle, Peter, A. and Dana, S. Ulmer-Scholle, 2003. A Color Guide to the Petrography of Carbonate Rocks: Grains, Textures, Porosity, Diagenesis, AAPG Memoir *77*. Vol.77. AAPG.

Scott, G.H., Nelson, C.S. and Stone, H.H., 1995. Planktic Foraminiferal Events in Early Miocene Zones N. 6 and N. 7 at Southwest Pacific DSDP Site 593: Relation with Climatic Changes in Oxygen Isotope Zone Milb. Marine Micropaleontology, Vol.25, No.1, p. 29 – 45.

Sharland, Peter R., David M. Casey, Roger B. Davies, Michael D. Simmons, and Owen E. Sutcliffe. 2004. Arabian Plate Sequence Stratigraphy – Revisions to SP2. GeoArabia, Vol.9, No.1, p. 199 – 214.

Shevenell, A.E., Kennett, J.P. and Lea, D.W., 2008. Middle Miocene Ice Sheet Dynamics, Deep-Sea Temperatures, and Carbon Cycling: A Southern Ocean Perspective. Geochemistry, Geophysics, Geosystems, Vol.9, No.2. DOI: 10.1029/2007GC001736.

Shevenell, Amelia E., James P. Kennett, and David W. Lea. 2004. Middle Miocene Southern Ocean Cooling and Antarctic Cryosphere Expansion. Science, Vol.305, No.5691, p.70 – 1766. DOI: 10.1126/science.1100061.

Smart, C.W. and Murray, J.W., 1994. An Early Miocene Atlantic-Wide Foraminiferal/Palaeoceanographic Event. Paleogeography, Palaeoclimatology, Palaeoecology, Vol.108, No. 1 – 2, p. 48 – 139.

Sosdian, S.M., Babila, T.L., Greenop, R., Foster, G.L. and Lear, C.H., 2020. Ocean Carbon Storage across the Middle Miocene: A New Interpretation for the Monterey Event. Nature Communications, Vol.11, No.1, p. 1 – 11.

Swart, Peter, K and Eberli, Gregor, P., 2005. Mean carbon-isotopic composition and standard deviations of deposition sequences of the Bahama Bank. PANGAEA, https://doi.org/10.1594/PANGAEA.763536,

Terwindt, J.H.J., 1988. Palaeo-Tidal Reconstructions of Inshore Tidal Depositional Environments. Tide-Influenced Sedimentary Environments and Facies, p. 63 – 233.

Vincent, Edith, and Wolfgang H. Berger, 1985. Carbon Dioxide and Polar Cooling in the Miocene: The Monterey Hypothesis. The Carbon Cycle and Atmospheric CO2: Natural Variations Archean to Present, Vol.32, p. 68 – 455.

Weissert, Helmut, and Elisabetta Erba, 2004. Volcanism, CO_2 and Palaeoclimate: A Late Jurassic – Early Cretaceous Carbon and Oxygen Isotope Record. Journal of the Geological Society, Vol.161, No.4, p. 695 – 702.

Westerhold, Thomas, Torsten Bickert, and Ursula Röhl, 2005. Middle to Late Miocene Oxygen Isotope Stratigraphy of ODP Site 1085 (SE Atlantic): New Constrains on Miocene Climate Variability and Sea-Level Fluctuations. Palaeogeography, Palaeoclimatology, Palaeoecology, Vol.217, No. 3 – 4, p. 22 – 205.

Woodruff, Fay and Samuel Savin. 1991. Mid- Miocene Isotope Stratigraphy in the Deep Sea: High- resolution Correlations, Paleoclimatic Cycles, and Sediment Preservation. Paleoceanography, Vol.6, No.6, p. 755 – 806. doi: 10.1029/91PA02561.

Woodruff, Fay, and Samuel M. Savin. 1989. Miocene Deepwater Oceanography. Paleoceanography, Vol.4, No.1, p. 87 – 140.

Wright, J.D., Miller, K.G. and Fairbanks, R.G., 1992. Early and Middle Miocene Stable Isotopes: Implications for Deepwater Circulation and Climate. Paleoceanography, Vol.7, No.3, p. 89 – 357. doi: 10.1029/92PA00760.

Wilson, J.L., 2012. Carbonate facies in geologic history. Springer Science and Business Media.

Zachos, J.C., Dickens, G.R. and Zeebe, R.E., 2008. An Early Cenozoic Perspective on Greenhouse Warming and Carbon-Cycle Dynamics. Nature, Vol.451, No.7176, p. 279 – 83. doi: 10.1038/nature06588.

Zachos, James, Mark Pagani, Lisa Sloan, Ellen Thomas, and Katharina Billups. 2001. Trends, Rhythms, and Aberrations in Global Climate 65 Ma to Present. Science, Vol.292, No.5517, p. 93 – 686.